doi:10.1038/nature11910

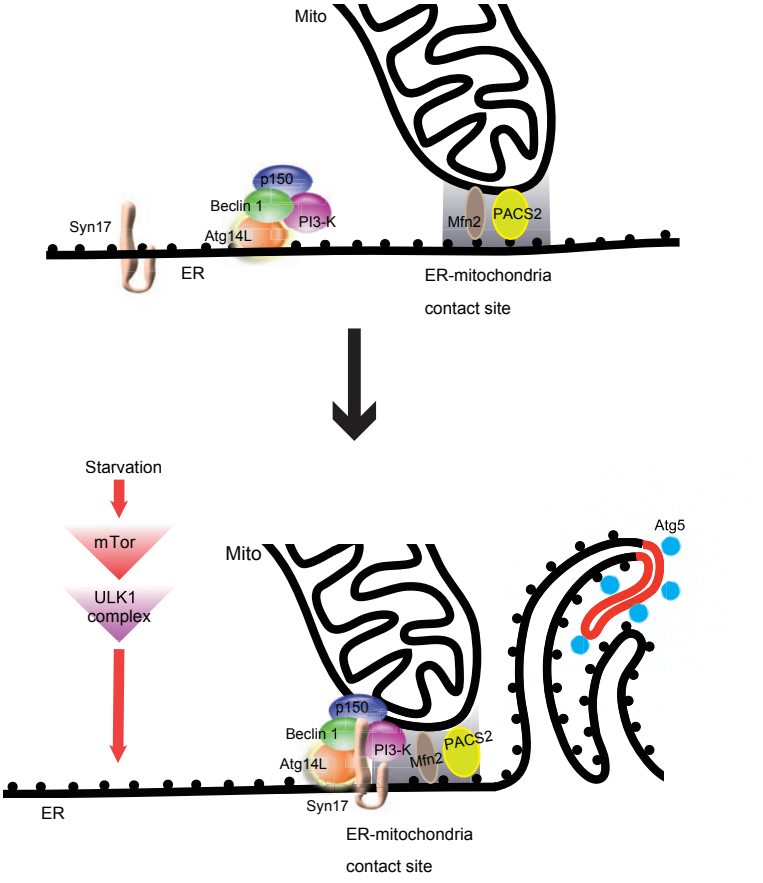

Supplementary Figure 1 | Model of autophagosome formation at the ER-mitochondria contact site.

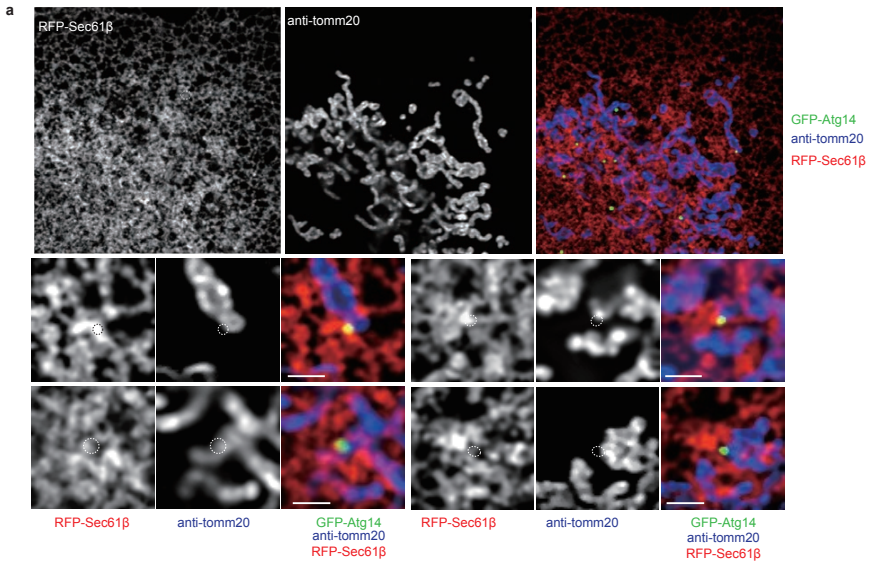

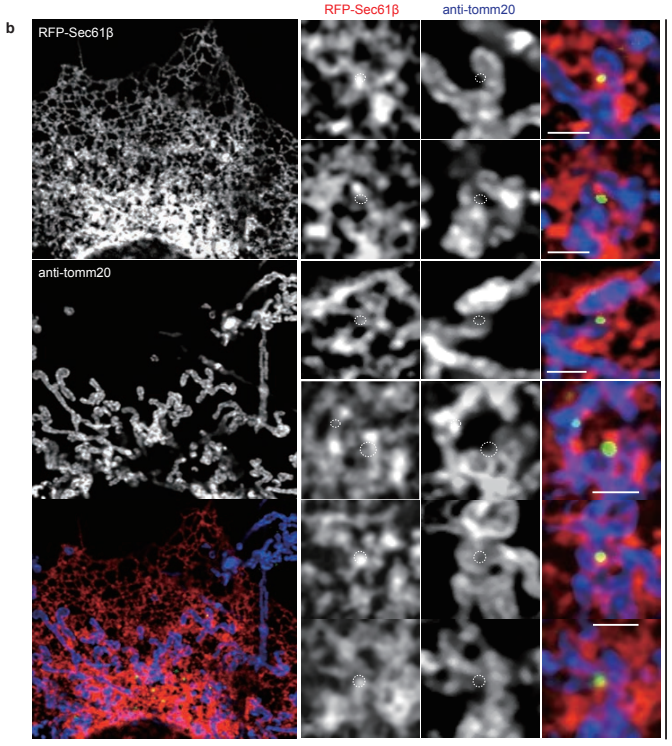

c

localization of Atg5 dots	n=356
adjacent or on both ER and Mt	188 (52.8%)
adjacent or on ER only	168 (47.2%)
adjacent or on Mt only	0 (0%)
on neither organelle	0 (0%)

Supplementary Figure 2 | Atg14 assembly and isolation membrane formation takes place at ER-mitochondria contact sites. a, COS7 cells co-transfected with GFP-Atg14L and RFP-Sec61b were immunostained for TOMM20 (a mitochondria marker) under starved conditions (2 h). **b,** COS7 cells stably expressing YFP-Atg5 (an isolation membrane marker) were transfected with RFP-Sec61β (ER marker) and were immunostained for TOMM20 (a mitochondria marker) under starved conditions (2 h). Scale bars, 2 μm. **c,** Quantification of localizations of YFP-Atg5 dots shown in **b**.

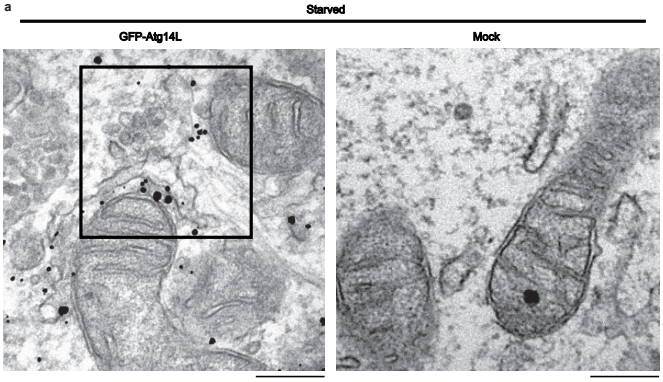

b

compartment	n	L (um)	LD, n/L
ER	50	22.0	2.3
Mt	26	42.9	0.6
ER-Mt contact site	126	9.8	12.9

n = observed golds
L = measured lengths
LD = labelling density

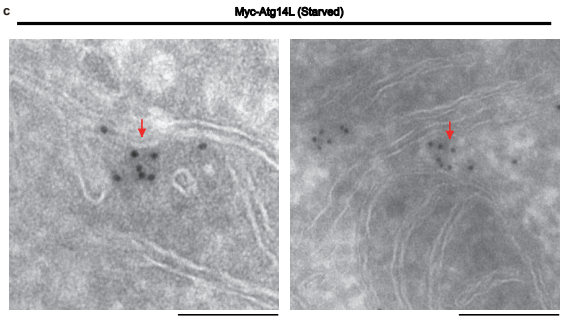

d

Compartment	Observed golds, n	Measured lengths (mm), L	LD, n/L
ER	40	74.102	0.540
Mt	2	49.842	0.040
ER-Mt contact site	58	16.742	3.464

Supplementary Figure 3 | Atg14L resides at ER-mitochondria contact site under starvation condition. a, HeLa cells expressing GFP-Atg14L under starvation for 2 h were microscopically probed with anti-GFP antibodies. Red arrows indicate immunogold-labeled GFP-Atg14L. Box indicate the Figure 1b. Scale bar, 200 nm. **b**, Quantification of Figure **1c** from 10 cells. **c**, HeLa cells were transfected with Myc-Atg14. After 24 h, the cells were starved for 2 h and analyzed microscopically using antibodies against Myc. Scale bars, 200 nm. **d**, Gold labeling of organelles of b. 15 sections were counted. LD, labeling density; Mt, Mitochondria.

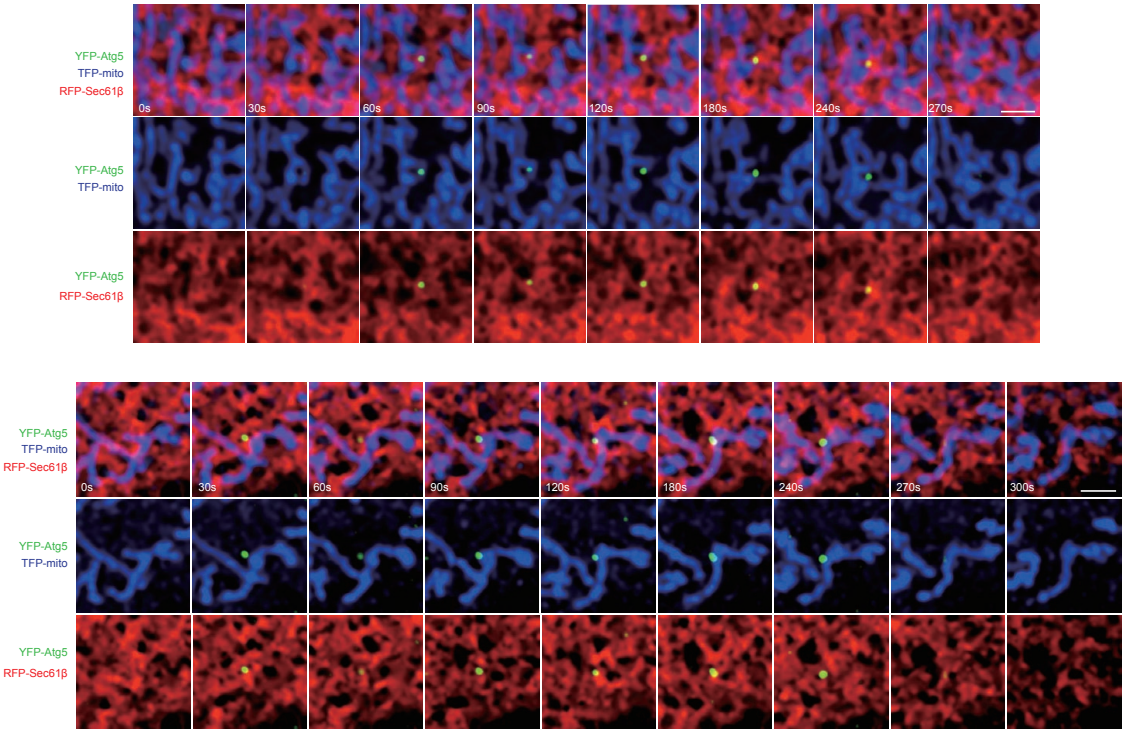

Supplementary Figure 4 | Isolation membrane formation takes place at the ER-mitochondria contact site. Time-lapse images of COS7 cells trasfected with YFP-Atg5, RFP-Sec61β and TFP-mito under starved conditions. Images were taken after cells were starved for one hour. Three channels were observed simultaneously using three cameras. Scale bars, 2 μm.

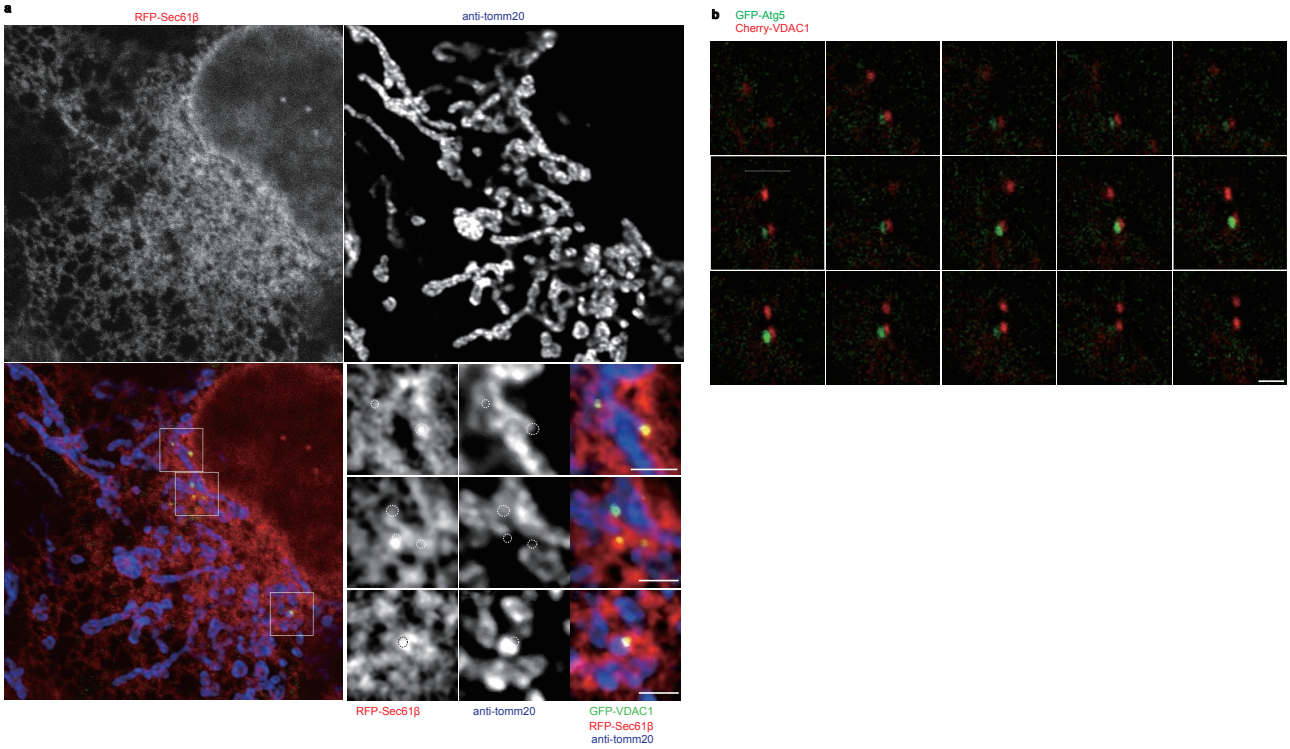

Supplementary Figure 5 | GFP-Atg5 puncta tightly interact with the Cherry-VDAC1, a marker of the ER-mitochondria contact site. a, Overexpressed Cherry-VDAC1 located at the ER-mitochondira contact site. COS7 cells transfected with GFP-VDAC1 and RFP-Sec61b were immunostained for TOMM20 (a mitochondria marker). **b,** Time-lapse images of HeLa cells stably expressing GFP-Atg5 and transiently expressing Cherry-VDAC1 under starved conditions. Live-cell images were taken after cells were incubated under the starved condition for 4.5 h; representative still frames are shown. Supplementary Figs 5b is frames from Supplementary movie 4. Scale bars, 2 μm

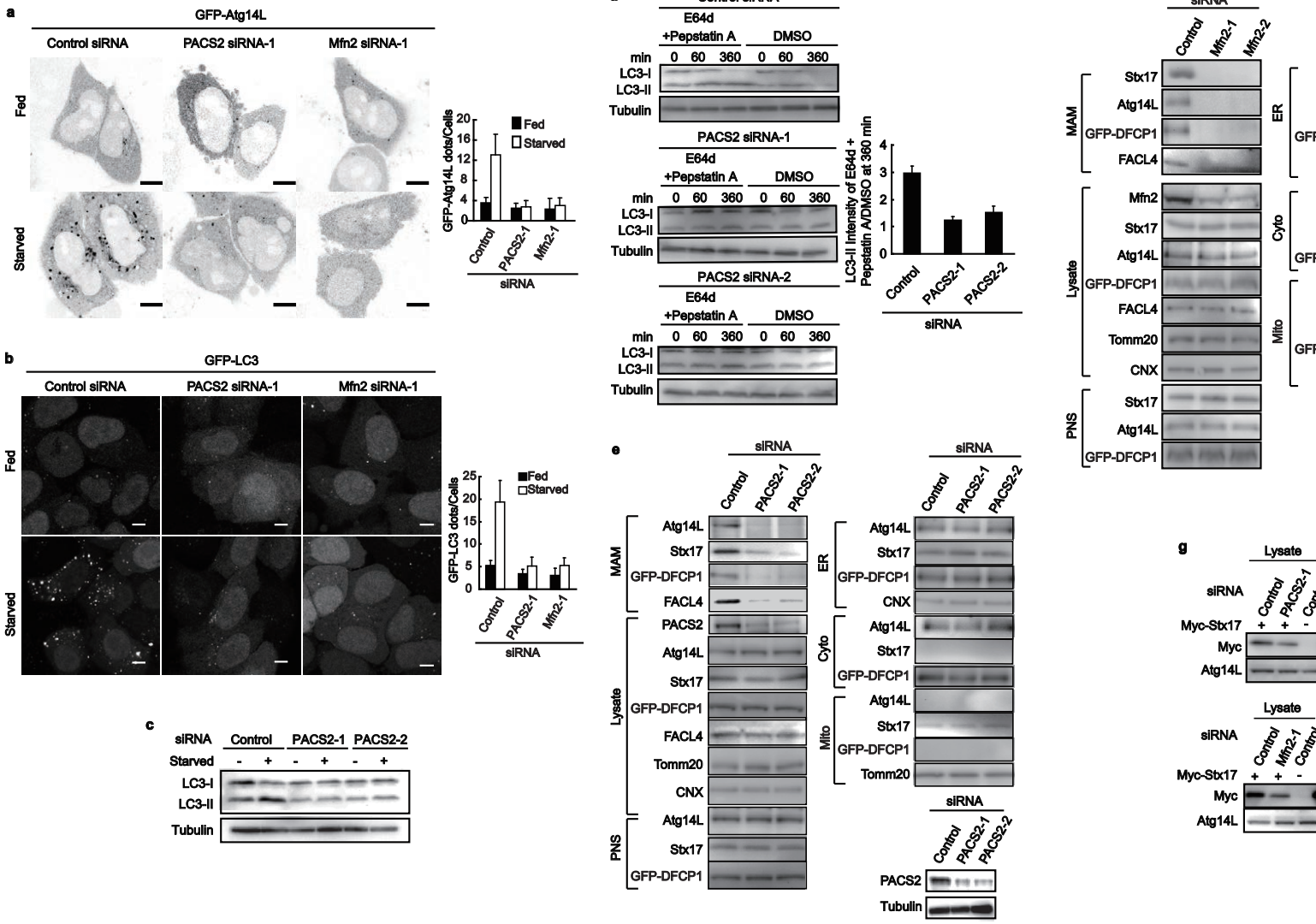
a
GFP-Atg14L
Control siRNA
PACS2 siRNA-1
Mfn2 siRNA-1
Fed
Starved
GFP-Atg14L dots/Cells
Fed
Starved
Control
PACS2-1
Mfn2-1
siRNA
b
GFP-LC3
Control siRNA
PACS2 siRNA-1
Mfn2 siRNA-1
Fed
Starved
GFP-LC3 dots/Cells
Fed
Starved
Control
PACS2-1
Mfn2-1
siRNA
c
siRNA
Control
PACS2-1
PACS2-2
Starved
LC3-I
LC3-II
Tubulin
d
Control siRNA
E64d
+Pepstatin A
DMSO
min
0 60 360 0 60 360
LC3-I
LC3-II
Tubulin
PACS2 siRNA-1
PACS2 siRNA-2
LC3-II Intensity of E64d + Pepstatin A/DMSO at 360 min
Control
PACS2-1
PACS2-2
siRNA
e
siRNA
Control
PACS2-1
PACS2-2
MAM
Atg14L
Stx17
GFP-DFCP1
FACL4
Lysate
PACS2
Tomm20
CNX
PNS
ER
Cyto
Mito
PACS2
Tubulin
f
siRNA
Control
Mfn2-1
Mfn2-2
MAM
Stx17
Atg14L
GFP-DFCP1
FACL4
ER
CNX
Lysate
Mfn2
Cyto
Mito
Tomm20
PNS
Mfn2
Tubulin
g
Lysate
IP:Myc-Stx17
siRNA
Control
PACS2-1
Control
Myc-Stx17
Myc
Atg14L
Mfn2-1

Supplementary Figure 6 | PACS2 and Mfn2-knockdown inhibit formation of ER-mitochondria contact sites and puncta formation of GFP-Atg14L and GFP-LC3 in starved cells. a, HeLa cells expressing GFP-Atg14L were transfected with siRNA against PACS2 or Mfn2. Cells were subjected to fed or starved conditions for 2 h and observed. The number of GFP-Atg14L puncta were counted (n>20 cells). **b,** PACS2 or Mfn2-knockdown HeLa cells expressing GFP-LC3 were subjected to fed or starved conditions for 2 h and observed. The number of GFP-LC3 puncta were counted (n=20 cells). **c,** PACS2-knockdown HeLa cells were starved and subjected to immunoblotting using antibodies against LC3 and tubulin. **d,** PACS2-knockdown HeLa cells were starved with or without proteinase inhibitors for the indicated times (minutes). Cell lysates were probed with antibodies against LC3 and tubulin. LC3-II proteins were gradually degraded in the control, indicating autophagic flux; lysosomal protease inhibitors (E64d and pepstatin A) prevented this degradation, with negligible effects on LC3-I. No flux-related degradation was observed in PACS2-knockdown cells. HeLa cells were transfected with siRNA against **e,** PACS2 or **f,** Mfn2. After 48 h, the cells were lysed and subjected to immunoblotting using specific antibodies. **g,** PACS2 or Mfn2-knockdown HeLa cells expressing Myc-Stx17 were immunoprecipitated by myc-antibodies and immunostained by antibodies indicated on the left.

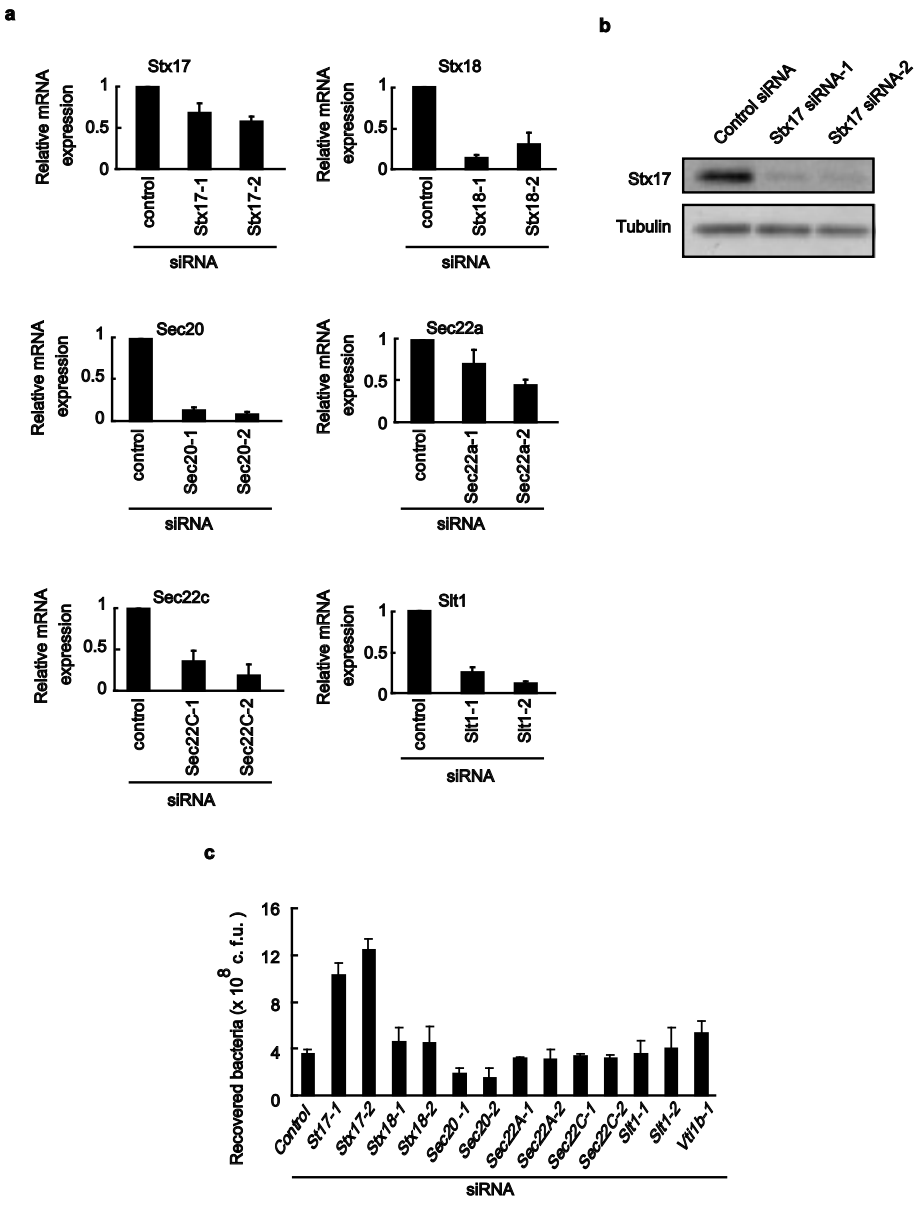

Supplementary Figure 7 | Effects of SNARE knockdown on autophagy against invading GAS. a, HeLa cells were transfected with siRNA against Stx17, Syntaxin 18, Sec20, Sec22a, Sec22c, Slt1 or a control siRNA. Real-time PCR analysis showed that the expression of these SNARE mRNA was successfully suppressed in HeLa cells. **b,** Stx17 protein expression was examined in siRNA knockdown HeLa cells by immunoblotting using antibodies against Stx17 and tubulin. c, HeLa cells were transfected with siRNA against various SNAREs. Cells were infected with GAS, and viable intracellular bacteria were counted in triplicate.

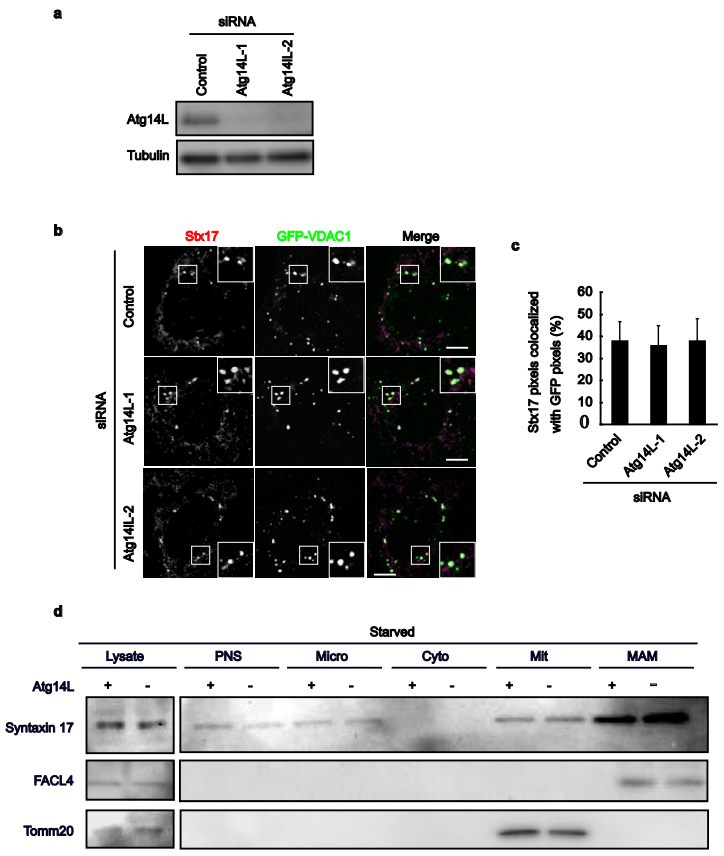

Supplementary Figure 8 | Negligible effects of Atg14L knockdown or knockout on assembly and localization of Stx17. a, Atg14L protein expression was examined in siRNA-knockdown HeLa cells by immunoblotting using antibodies against Atg14L and tubulin. **b,** Atg14L-knockdown HeLa cells expressing Cherry-VDAC1 were starved for 2 h and probed with antibodies against Stx17. **c,** Colocalization of Stx17 and GFP-VDAC1 of b (mean ± SD, > 20 cells for each sample, Zeiss LSM Image Browser software). **d,** Atg14L-knockout and WT MEFs were subjected to starved conditions and probed by Western blotting using antibodies against Stx17, FACL4 and TOMM20. Scale bars, 5 μm.

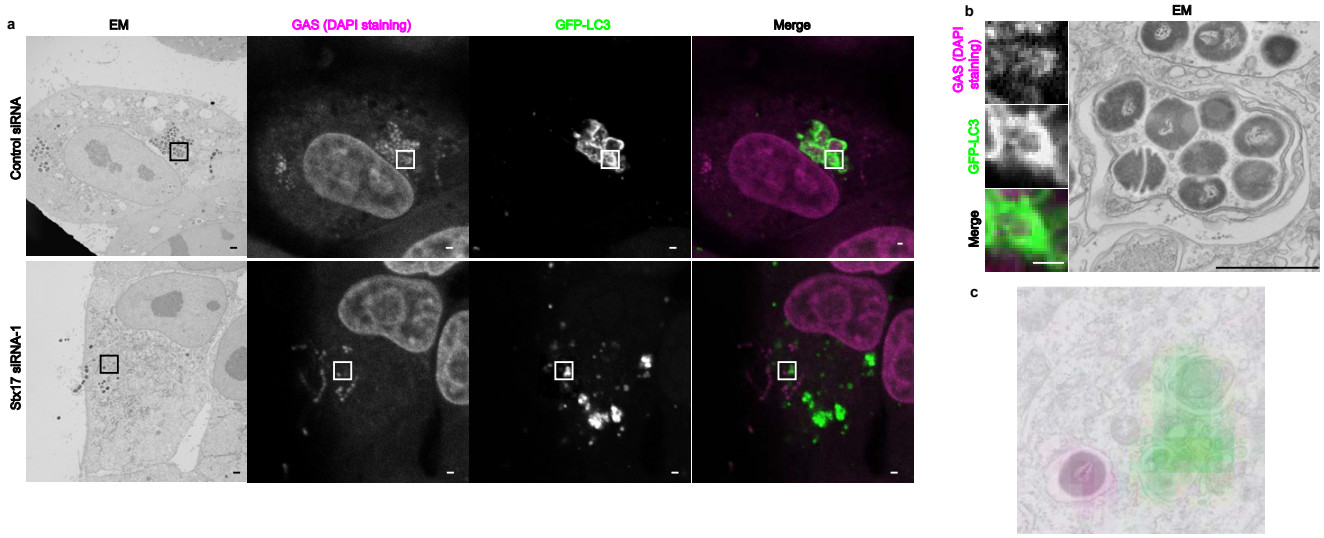

Supplementary Figure 9 | The formation of xenophagosomes is attenuated in Stx17-knockdown cells. a, HeLa cells stably expressing GFP-LC3 were transfected with siRNAs against Stx17. The cells were infected with GAS for 1 hour. DNA was stained by DAPI. **b,** Cropped image of a. **c,** Overlapped image of light and electron microscopy of Stx17 knockdown cell of Figure 4a. Scale bars, 5 μm.

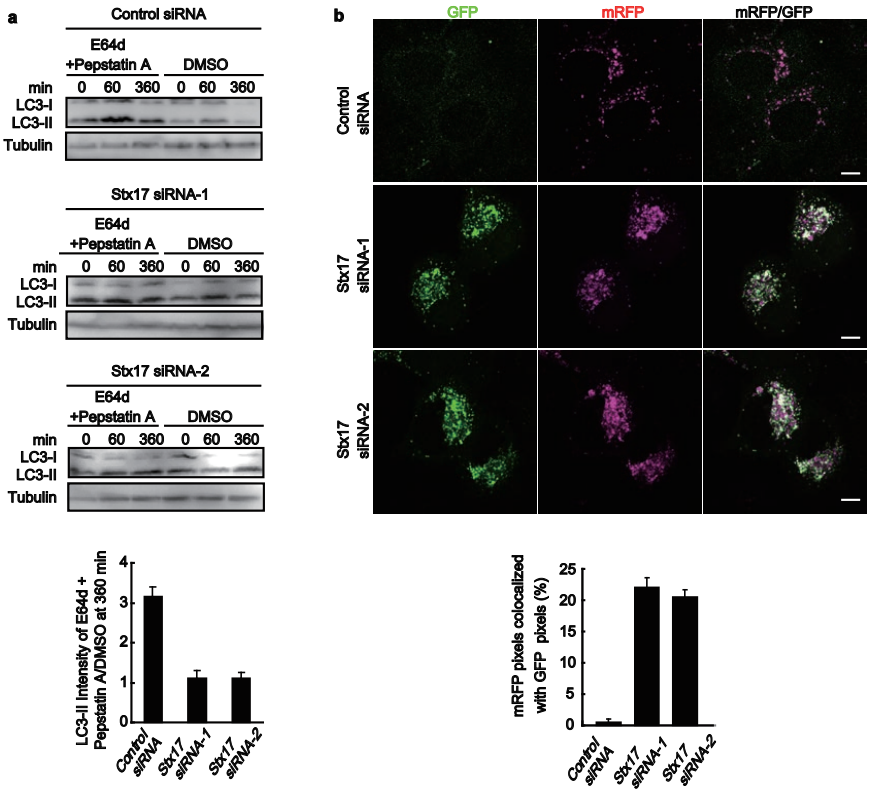

Supplementary Figure 10 | Effects of Stx17-knockdown on autophagosome formation. a, Autophagic flux was examined on Stx17-knockdown HeLa cells starved with or without proteinase inhibitors for the indicated times (min). Cell lysates were probed with antibodies against LC3 and tubulin. LC3-II protein levels gradually decreased in the control, indicating autophagic flux; lysosomal protease inhibitors (E64d and pepstatin A) prevented this degradation, with negligible effect on LC3-I. No flux-related degradation was observed in Stx17-knockdown cells. Relative intensities of LC3-II bands (inhibitor treated/control) at 360 min were measured and ploted from three independent experiments. **b,** mRFP-GFP tandem−tagged LC3 (tfLC3) was used to distinguish autophagic vacuoles; mRFP(+)GFP(+)-LC3 spots represent autophagosomes and their precursors, whereas mRFP(+)GFP(−)-LC3 spots indicate autolysosomes (the GFP signal is susceptible to lysosomal degradation, whereas mRFP is resistant). The puncta of both LC-3 markers were clearly merged in Stx17-knockdown cells, indicating impairment of autophagic degradation. Colocalization of mRFP with GFP signals are plotted in pixels (> 30 cells/sample) Scale bars, 5 μm.